AFOSR-TR- 77-0777

12 B.S.

*Interim Report 2*

*May 1977*

# ANALYSIS OF RADAR DETECTION OF AGITATED METALS (RADAM)

*By:* A. J. BAHR J. P. PETRO L. E. SWEENEY, JR.

*Prepared for:*

AIR FORCE OFFICE OF SCIENTIFIC RESEARCH
DIRECTORATE OF ELECTRONIC AND
SOLID STATE SCIENCES
BOLLING AIR FORCE BASE, BUILDING 410
WASHINGTON, D.C. 20332

Attention: DR. GEORGE E. KNAUSENBERGER
PROGRAM MANAGER, AFOSR/NE

CONTRACT F44620-75-C-0046

Approved for Public Release; Distribution Unlimited.



SRI
STANFORD RESEARCH INSTITUTE
Menlo Park, California 94025 · U.S.A.

# DISCLAIMER NOTICE

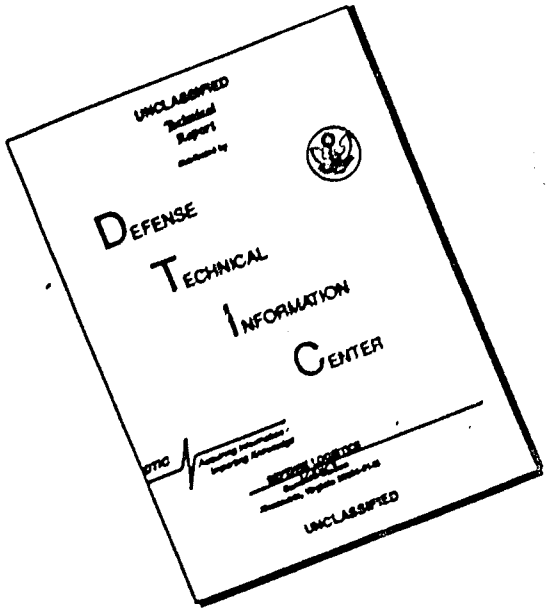


THIS DOCUMENT IS BEST QUALITY AVAILABLE. THE COPY FURNISHED TO DTIC CONTAINED A SIGNIFICANT NUMBER OF PAGES WHICH DO NOT REPRODUCE LEGIBLY.

The research reported herein was sponsored by the Air Force Office of Scientific Research (AFSC), United States Air Force, under Contract F44620-75-C-0046. The United States Government is authorized to reproduce and distribute reprints for governmental purposes notwithstanding any copyright notation hereon.

UNCLASSIFIED

SECURITY CLASSIFICATION OF THIS PAGE (When Data Entered)

## REPORT DOCUMENTATION PAGE

READ INSTRUCTIONS BEFORE COMPLETING FORM

1. REPORT NUMBER: AFOSR-TR-77-0777
2. GOVT ACCESSION NO.
3. RECIPIENT'S CATALOG NUMBER

4. TITLE (and Subtitle): ANALYSIS OF RADAR DETECTION OF AGITATED METALS (RADAM)

5. TYPE OF REPORT & PERIOD COVERED: Interim rept. no. 2 (FINAL), 1 Apr 76–31 Mar 77

6. PERFORMING ORG. REPORT NUMBER: SRI Project 4176

7. AUTHOR(s): A. J. Bahr, J. P. Petro, L. E. Sweeney, Jr.

8. CONTRACT OR GRANT NUMBER(s): Contract F44620-75-C-0046

9. PERFORMING ORGANIZATION NAME AND ADDRESS: Stanford Research Institute, Menlo Park, California 94025

10. PROGRAM ELEMENT, PROJECT, TASK AREA & WORK UNIT NUMBERS: 61102F / 2305/B2

11. CONTROLLING OFFICE NAME AND ADDRESS: Air Force Office of Scientific Research (AFOSR/NE), Bldg. 410, Bolling AFB, Washington, D.C. 20332

12. REPORT DATE: May 1977

13. NO. OF PAGES: 44

14. MONITORING AGENCY NAME & ADDRESS (if diff. from Controlling Office)

15. SECURITY CLASS. (of this report): UNCLASSIFIED

15a. DECLASSIFICATION/DOWNGRADING SCHEDULE: N/A

16. DISTRIBUTION STATEMENT (of this report)

Approved for Public Release; Distribution Unlimited.

17. DISTRIBUTION STATEMENT (of the abstract entered in Block 20, if different from report)

18. SUPPLEMENTARY NOTES

19. KEY WORDS (Continue on reverse side if necessary and identify by block number)

Radar scattering
Intermittent contacts
Loaded scatterers

20. ABSTRACT (Continue on reverse side if necessary and identify by block number)

We have shown that switching of the target surface currents established by an illuminating radar is the basic physical mechanism that is operative in intermittent-contact RADAM. These varying surface currents produce both amplitude and phase modulation of the scattered signal. In this report we discuss the questions of frequency dependence, contact location and phasing, contact coherence, target-element motion, and contact materials as they relate to intermittent-contact RADAM.

332500

DD FORM 1 JAN 73 1473
EDITION OF 1 NOV 65 IS OBSOLETE

UNCLASSIFIED
SECURITY CLASSIFICATION OF THIS PAGE (When Data Entered)

STANFORD RESEARCH INSTITUTE
Menlo Park, California 94025 · U.S.A.

*Interim Report 2*
*Covering the Period 1 April 1976 to 31 March 1977*

*May 1977*

# ANALYSIS OF RADAR DETECTION OF AGITATED METALS (RADAM)

*By:* A. J. BAHR J. P. PETRO L. E. SWEENEY, JR.

*Prepared for:*

AIR FORCE OFFICE OF SCIENTIFIC RESEARCH
DIRECTORATE OF ELECTRONIC AND
SOLID STATE SCIENCES
BOLLING AIR FORCE BASE, BUILDING 410
WASHINGTON, D.C. 20332

Attention: DR. GEORGE E. KNAUSENBERGER
PROGRAM MANAGER, AFOSR/NE

CONTRACT F44620-75-C-0046

SRI Project 4176

Approved for Public Release; Distribution Unlimited.

*Approved by:*

RAY L. LEADABRAND, *Executive Director*
*Electronics and Radio Sciences Division*



*Copy No.* 4

CONTENTS

ILLUSTRATIONS

TABLE

# I INTRODUCTION

It has been observed that the radar returns from moving multielement metal targets often exhibit an unexpected modulation that has both random (or noise-like) and semicoherent components. One possible mechanism for producing this effect is the modification of the current distribution on the target that results when electrical contacts between target elements are altered intermittently by the forces associated with target motion. Such intermittent-contact modulation must be considered in the design of a radar for detecting or identifying a target exhibiting this effect. Depending on the application, the observer may wish to enhance or suppress the observation of the effect, or it may be important that the effect itself be enhanced or suppressed in the object being observed. To accomplish any of these, the effect must be well understood, and we have therefore undertaken a program of research to study the radar detection of agitated metals (RADAM). This report summarizes our progress during the second year of the program.

The overall objectives of our RADAM research program are to (1) identify and isolate the physical processes and mechanisms that contribute to a RADAM signature, (2) identify and explain important recognizable features of the signature, and (3) determine means for separating the significant identifying components of the signature from nonmeaningful components.

To date, the following publications have resulted from this work:

- A. J. Bahr, V. R. Frank, J. P. Petro, and L. E. Sweeney, Jr., "Radar Scattering from Intermittently Contacting Metal Targets," IEEE Trans. on Antennas and Propagation (to be published in July 1977).
- V. R. Frank, J. P. Petro, and A. J. Bahr, "Backscattering from a Cylindrical Dipole Centrally Loaded by a Time-Varying Impedance," IEEE Trans. on Antennas and Propagation, Vol. AP-25, pp. 356-358 (May 1977).

- A. J. Bahr and J. P. Petro, "On the RF Frequency Dependence of the Scattered Spectral Energy Produced by Intermittent Contacts Among Elements of a Target," to be submitted for publication. This paper will also be given orally at the 1977 International IEEE APS Symposium, Stanford, Calif., June 20-24, 1977.

## II SUMMARY OF PROGRESS

During the first year of this study we were successful in identifying the basic physical mechanism that is operative in intermittent-contact RADAM as being the switching of the surface currents that are established on the target by the illuminating radar. These varying surface currents produce both amplitude and phase modulation of the scattered signal. The characteristics of this modulation depend on the impedances associated with the open and closed states of the contacts, the contact bounce, the location of the contacts on the target, and the degree of coherence between the contact motions. In general, we have found that a target having contacts can be modeled as a loaded scatterer, where each contact is represented by a particular load impedance. The concept of impedance is applicable to this dynamic situation because the frequency of contact modulation in most real targets is slow compared with the RF transient response of the target.

Our work during the second year has been concerned with the questions of the frequency dependence of the intermittent-contact RADAM effect, contact location and phasing, contact coherence, distinguishing intermittent-contact RADAM from the scattering modulation produced by motion of the target elements, and of the effect of contact materials.

### A. Frequency Dependence of Intermittent-Contact RADAM

In general, the frequency dependence of the intermittent-contact modulation associated with a complex target will be determined by the surface-current distribution on the target with all contacts short circuited, the number and placement of the contacts, and the impedances of the open and closed contacts. In principle, a target having intermittent contacts can be represented by a multiport loaded-scatterer model[1]* and

*References are listed at the end of this report.

can be analyzed using numerical methods. However, a basic understanding of the problem can be obtained by considering a simple target having only a single contact (port) that can be studied using relatively simple analytical and experimental techniques.

Hence, we have chosen to study the RF frequency dependence of the backscattering from a dipole loaded at its center by a vibrating-reed switch.

Backscattering from a center-loaded cylindrical dipole has been considered theoretically by Hu.[2] He defines a two-port network composed of an infinitesimally small dipole probe and the loaded dipole that produces the scattering. The component of scattered electrical field that is sensed by the probe when it is aligned with the scattering dipole can then be written in terms of the Z matrix $[Z_{ij}]$ for the two-port network--viz.,

$$E^S(Z_L) = C\left[(Z_{11} - Z_1) - \frac{Z_{12}^2}{Z_{22} + Z_L}\right] \tag{1}$$

where C is a probe constant, $Z_1$ is the input impedance of the probe in the absence of the scatterer, and $Z_L$ is the impedance that loads the scattering dipole. It is convenient to write Eq. (1) in terms of the scattered electric field for $Z_L = 0$--i.e.,

$$E^S(Z_L) = E^S(0)\left[1 - \alpha\left(\frac{Z_L}{Z_L + Z_r}\right)\right] \tag{2}$$

where the coupling factor, $\alpha$, is defined as

$$\alpha = \frac{1}{1 - Z_r(Z_{11} - Z_1)/Z_{12}^2} \tag{3}$$

and $Z_r \approx Z_{22}$ is the radiation impedance of the scattering dipole. We note that the dependence of the scattering on $Z_L$ is contained entirely within the factor $Z_L/(Z_L + Z_r)$ in Eq. (2). It should also be noted that Eq. (2) is not restricted to a dipole, but holds for an arbitrary scatterer having a single loading port.

In order to study the frequency dependence of intermittent-contact modulation, we focus on the behavior of the power in the sidebands associated with the modulated signal. For simplicity, we assume that $Z_L$ varies in a periodic square-wave fashion between the two states defined by $Z_L = 0$ and $Z_L = Z_{LR}$. The scattered electric fields for these two states can be written in phasor notation as follows:

$$E^S(0) \equiv E_0 e^{j\phi_0} \tag{4a}$$

and

$$E^S(Z_{LR}) \equiv E_L e^{j\phi_L} \quad . \tag{4b}$$

If we apply standard Fourier analysis to the assumed square waveform and use Eq. (2), we obtain the following result for the power contained in the $n^{th}$ sideband:

$$P_n^{\pm} = P_0 \left[\frac{\sin n\pi f_d}{n\pi}\right]^2 \left|\frac{\alpha Z_{LR}}{Z_{LR} + Z_r}\right|^2 \quad . \tag{5}$$

In this equation, $P_0$ is the power scattered by the target when the contact is short-circuited; $n = 1, 2, 3, \ldots$ ; $f_d$ is the ratio of time the contact spends in the "zero" state to the period of the waveform; and the superscripts plus and minus refer to spectral frequencies above and below the carrier frequency, respectively. These spectral frequencies are separated from the carrier frequency by an amount n/T, where T is the period of the waveform.

We can identify the quantity $\alpha Z_{LR}/(Z_{LR}+Z_r)$ as a "RADAM factor" for this example. In general, both the amplitude and phase of this factor determine the spectra, but for this special case only the amplitude is important.

We see, then, that the dependence of $P_n$ on the RF carrier frequency is contained in three parameters: $P_0$, $\alpha$, and $Z_{LR}/Z_r$. For a dipole these parameters can be calculated easily using the results given by Hu.[2] We have calculated the frequency dependence of the radar cross section (RCS) of a specific dipole with a short-circuit load (proportional to $P_0$), and of the dipole's corresponding RADAM factor for square-wave modulation. These results are shown in Figures 1(a) and 1(b), respectively. The squared magnitude of the RADAM factor has been plotted for three different values of load capacitance, $C_{LR}$, assuming a purely capacitive load impedance. We see that the RADAM factor is quite sensitive to the value of $C_{LR}$.

The amplitude of the spectral power for square-wave modulation is proportional to the product of the reference RCS and the squared magnitude of the RADAM factor. Hence, since the ordinates in Figures 1(a) and 1(b) are in dB, they can be added to produce the net relative spectral power in dB as a function of RF carrier frequency. The result of carrying out this operation for the case $C_{LR}$ = 0.8 pF is shown in Figure 2. The double-peaked response observed near $f/f_0 = 1$ is the result of coupling between the resonances of the shorted and capacitively loaded dipoles, respectively.

The loaded-scatterer model predicts that, neglecting the frequency dependence of the contact impedance, the frequency dependence of the spectral power produced by intermittent-contact modulation is determined only by the ratio of the characteristic dimensions of the target to the wavelength. Further, the example of a dipole shows that the intermittent-contact effect is greatest at frequencies that produce resonances in the scatterer response--i.e., when the length of the dipole is approximately equal to an odd multiple of one-half wavelength. Although most scatterers do not exhibit resonances as strong as those of a dipole, they still

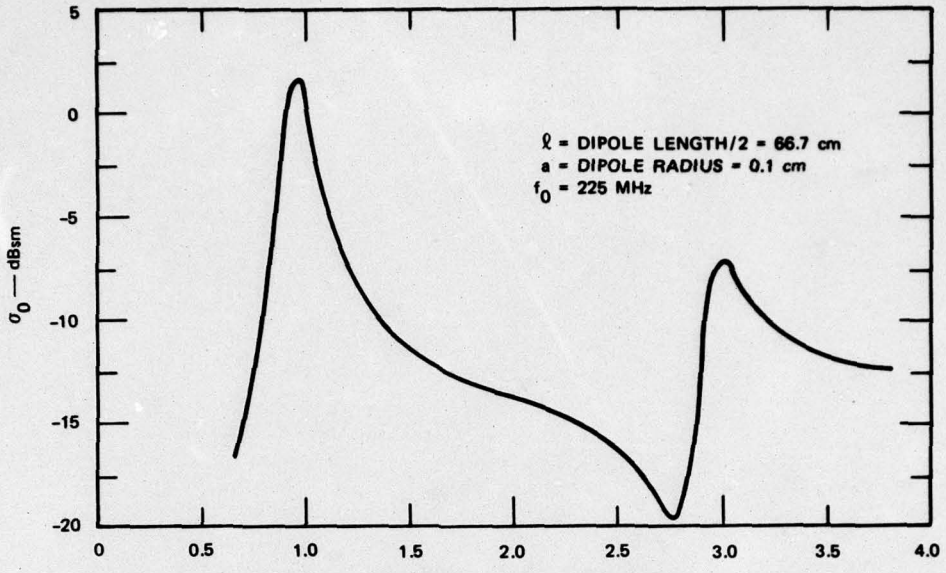


(a) RADAR CROSS SECTION FOR A SHORT-CIRCUIT LOAD

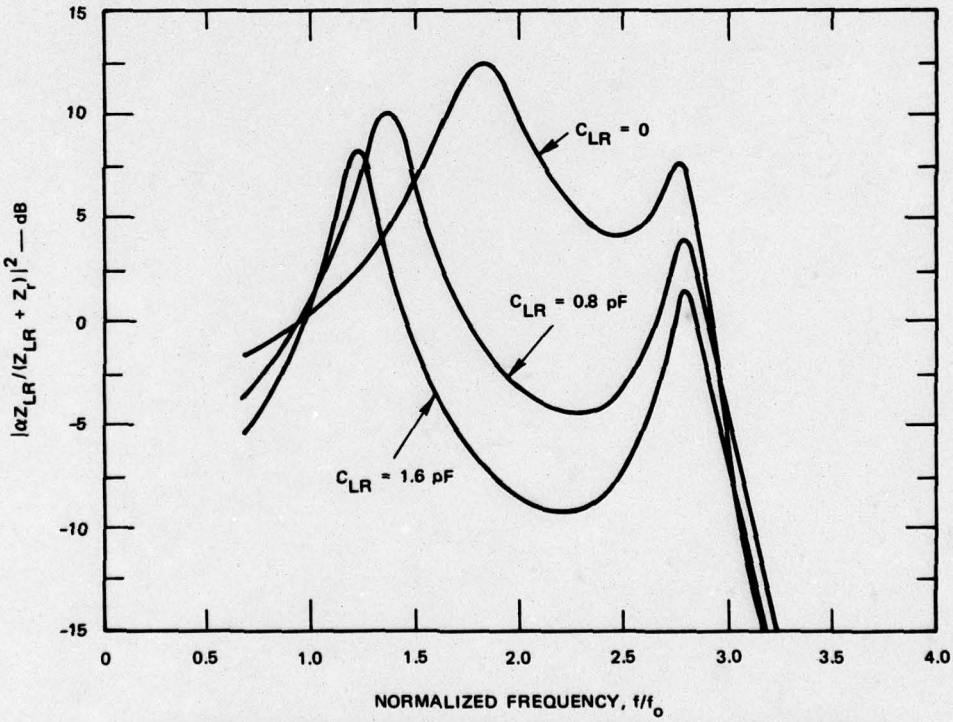


(b) RADAM FACTOR FOR SQUARE-WAVE MODULATION WITH LOAD CAPACITANCE AS A PARAMETER

SA-4176-2

FIGURE 1 FREQUENCY CHARACTERISTICS FOR A CENTRALLY LOADED DIPOLE

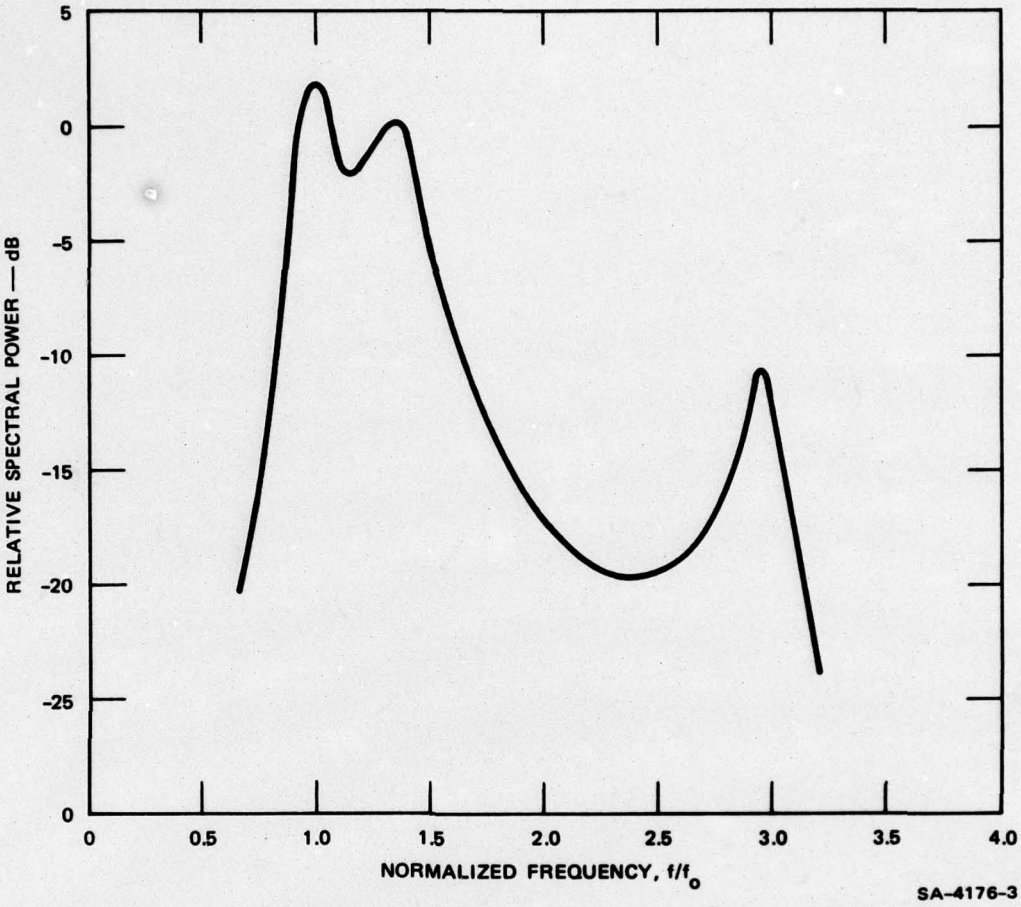


FIGURE 2 RELATIVE SPECTRAL POWER AS A FUNCTION OF NORMALIZED FREQUENCY FOR THE DIPOLE OF FIGURE 1 AND $C_{LR}$ = 0.8 pF

tend to exhibit the greatest RCS when their characteristic dimensions approximately satisfy the half-wavelength criterion (which dimensions are significant depends on the polarization and aspect angle of the incident radiation). Hence, this reasoning provides a guide for determining the operating frequency of a radar that is designed to maximize the detection of intermittent-contact effects--lower frequencies should be used for large targets and higher frequencies for small targets, the approximate required frequency band being calculable from the dimensions of the target. In practice, of course, there are other factors such as

the physical size of the antennas and the frequency dependence of the illumination for targets near the earth's surface that can have a significant effect on the choice of optimum radar frequency, and such factors must be considered in an overall system design.

An experiment was carried out to confirm the theoretically predicted frequency dependence of the RADAM factor for a dipole undergoing square-wave modulation. In addition, measurements were made using two dipoles of different size in order to demonstrate the frequency-scaling behavior of the RADAM factor.

The experimental procedure was as follows: a dipole centrally loaded by a reed switch [Hamlin-Mark 3] vibrating at 1 kHz was illuminated by a signal at a fixed RF frequency and the resulting backscattered signal was detected by a scanning spectrum analyzer. In order to eliminate the frequency dependence of the backscattering from a shorted dipole, the system gain was adjusted at each frequency so that the signal obtained with the reed switch closed was always at the same level on the logarithmic display of the spectrum analyzer. Then, the vertical displacement voltage in this display was integrated over a time that corresponded to an upper-sideband portion of the spectrum. By integration over several scans of the spectrum analyzer, this technique permitted a good signal-to-noise ratio to be obtained in the measurement. Finally, the resulting integrated voltage, $V_T$, was displayed on a digital voltmeter and recorded.

The scanning spectrum analyzer provided a convenient means for monitoring the received power and spectrum during the measurement. However, a disadvantage of this procedure was that the system could not be readily calibrated in terms of relative power because of the nonlinearity introduced when the response of the Gaussian IF filter in the spectrum analyzer (as modified by the limited dynamic range of the display) was integrated. The convenience of this measurement system outweighed this disadvantage, however, since our main objective was simply to illustrate the frequency behavior of the RADAM factor.

The experimental results for integrated voltage as a function of frequency are shown in Figure 3. In order to compare these results with

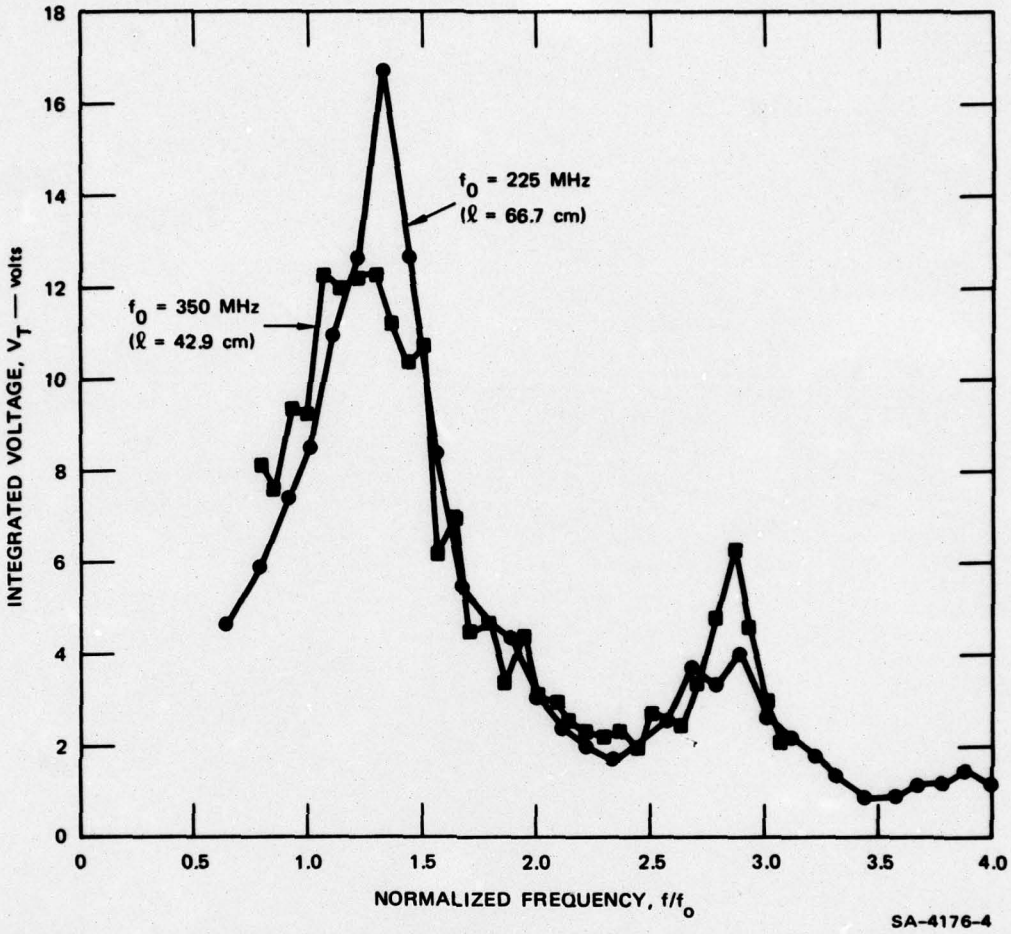


**FIGURE 3 MEASURED RELATIVE RADAM FACTOR AS A FUNCTION OF FREQUENCY FOR TWO DIFFERENT DIPOLES**

theory, we computed the corresponding RADAM factor for a number of different values of the load capacitance $C_{LR}$. The theoretical results that fit our data best, in terms of the frequencies where the peaks in the response occur, are shown in Figure 4. The agreement between theoretical and experimental peak positions is seen to be very good for the lower frequency peaks, and only in slight disagreement for the upper frequency peaks. This latter discrepancy is probably due to the neglect of the stray inductance of the reed switch in the model for $Z_{LR}$. The best-fit value of $C_{LR} \approx 0.9$ pF is not unreasonable for the reed switch that was

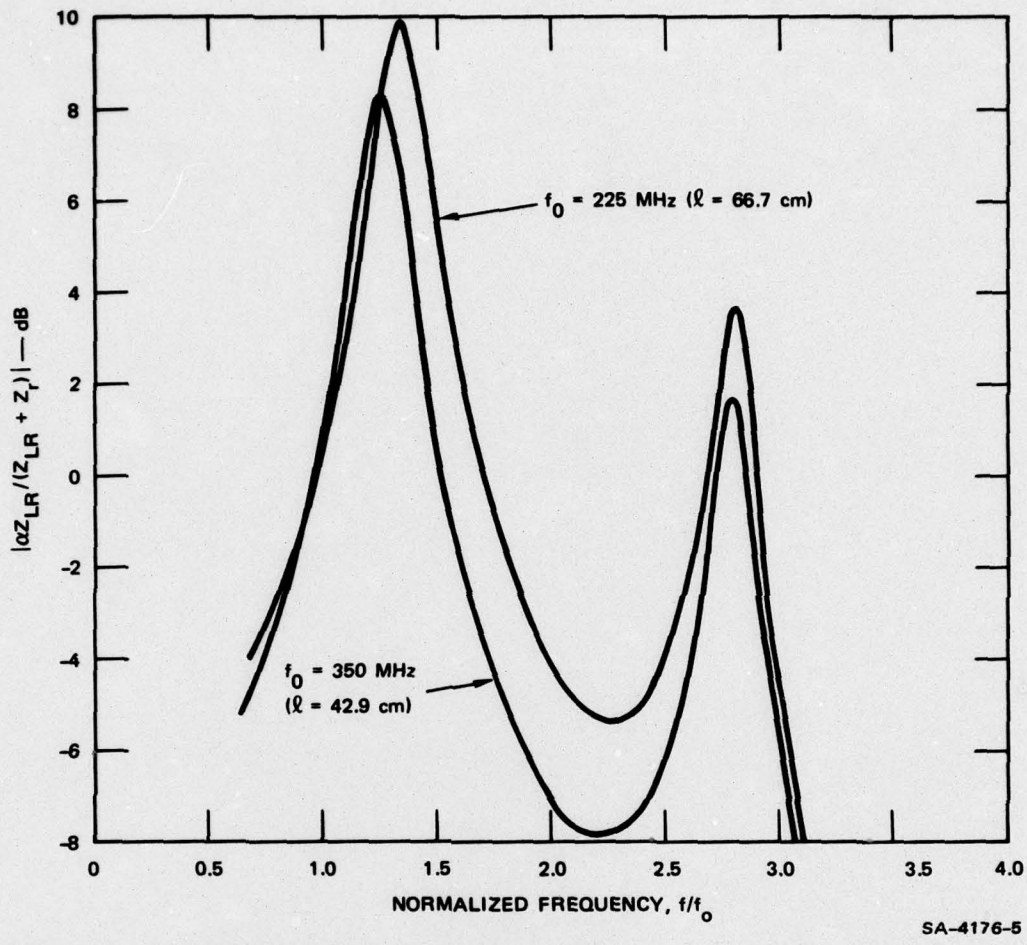


**FIGURE 4 THEORETICAL RADAM FACTOR AS A FUNCTION OF FREQUENCY FOR TWO DIFFERENT DIPOLES ($C_{LR}$ = 0.9 pF)**

used ($C_{reed}$ = 0.2 pF), when one considers that there is stray capacitance associated with the gap between the ends of the severed dipole. Finally, even though the vertical scale in Figure 3 is uncalibrated, we can say that the shapes of the experimental and theoretical curves are in qualitative agreement. In general, then, we conclude that the frequency-scaling behavior of the RADAM factor for a dipole agrees with the theoretical predictions.

In summary, we have shown that the spectral energy scattered from a single-load-port target loaded by a time-varying impedance is dependent

on the RF frequency of the incident wave. The three basic parameters describing this dependence are: (1) the scattering cross section of the short-circuited target, (2) a target- and radar-dependent coupling factor, and (3) the ratio of a reference load impedance to the radiation impedance of the target when it is excited at its load port. The first two of these parameters are independent of the reference load impedance, and thus are the same for two different targets having the same ratio of target dimensions to wavelength. However, if the reference load impedance is frequency-dependent, the third parameter will not possess this frequency-scaling property. This behavior has been illustrated theoretically and experimentally for a centrally loaded dipole undergoing square-wave modulation by a reed switch.

## B. Multiple-Contact Effects

Up to now our theory and experiments have dealt with situations involving only a single contact. However, in practice it is more likely that a target will possess more than one contact--in fact, usually there will be a large number of contacts if there are any at all. Hence, we have conducted several experiments that are designed to illustrate some of the effects that can result from the existence of multiple contacts on the target.

For these experiments, we chose a scatterer composed of two identical metal plates that were connected by three independently controlled reed switches. The plate configuration is illustrated in Figure 5. The two plates were separated by a small gap, and two switches were connected at opposite ends of the gap, with the third switch connected exactly in the middle of the gap. The two plates were illuminated in a broadside direction by a 350-MHz CW signal that was linearly polarized in a direction perpendicular to the long dimension of the gap separating the plates. At this frequency, the plates are each about one-quarter wavelength long in the direction of incident polarization.

In these experiments the received backscattered signal was band-limited to 1200 Hz, and sampled at 2400 Hz, and the result was recorded

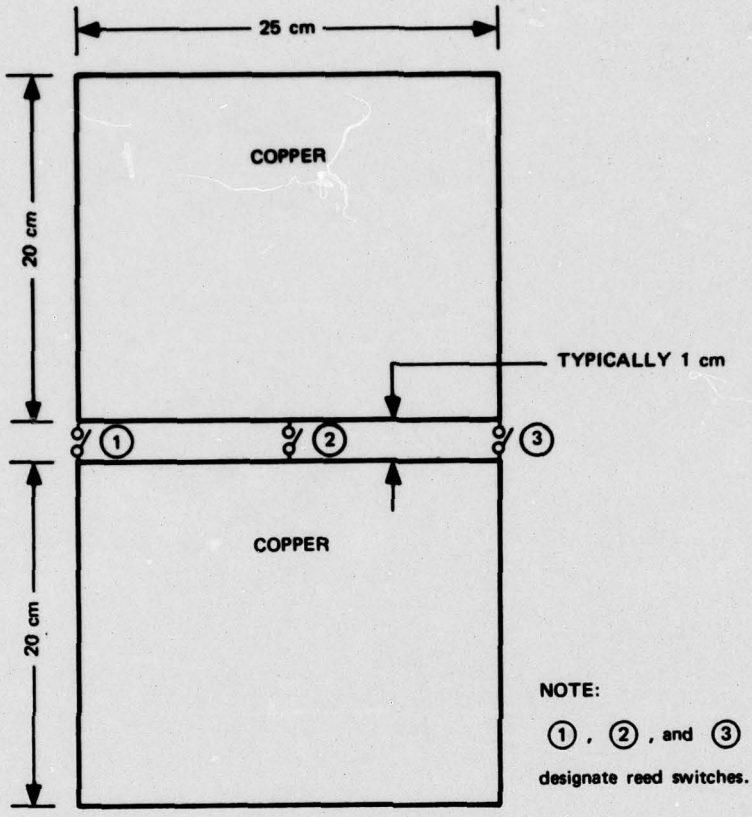


FIGURE 5 TWO-PLATE SCATTERER WITH MULTIPLE CONTACTS

on magnetic tape. Subsequent digital processing of the data provided displays of amplitude versus time, phase versus time, and the spectrum.

1. Effects of Contact Location

Experiments were conducted wherein one switch was activated at a time in order to study qualitatively the effects of switch location. The temporal and spectral characteristics of the modulated backscattered signals that were obtained in four different situations are shown in Figure 6. Because the switching waveform was a square wave with a 50% duty cycle, only the odd harmonics of the 10-Hz switching rate are

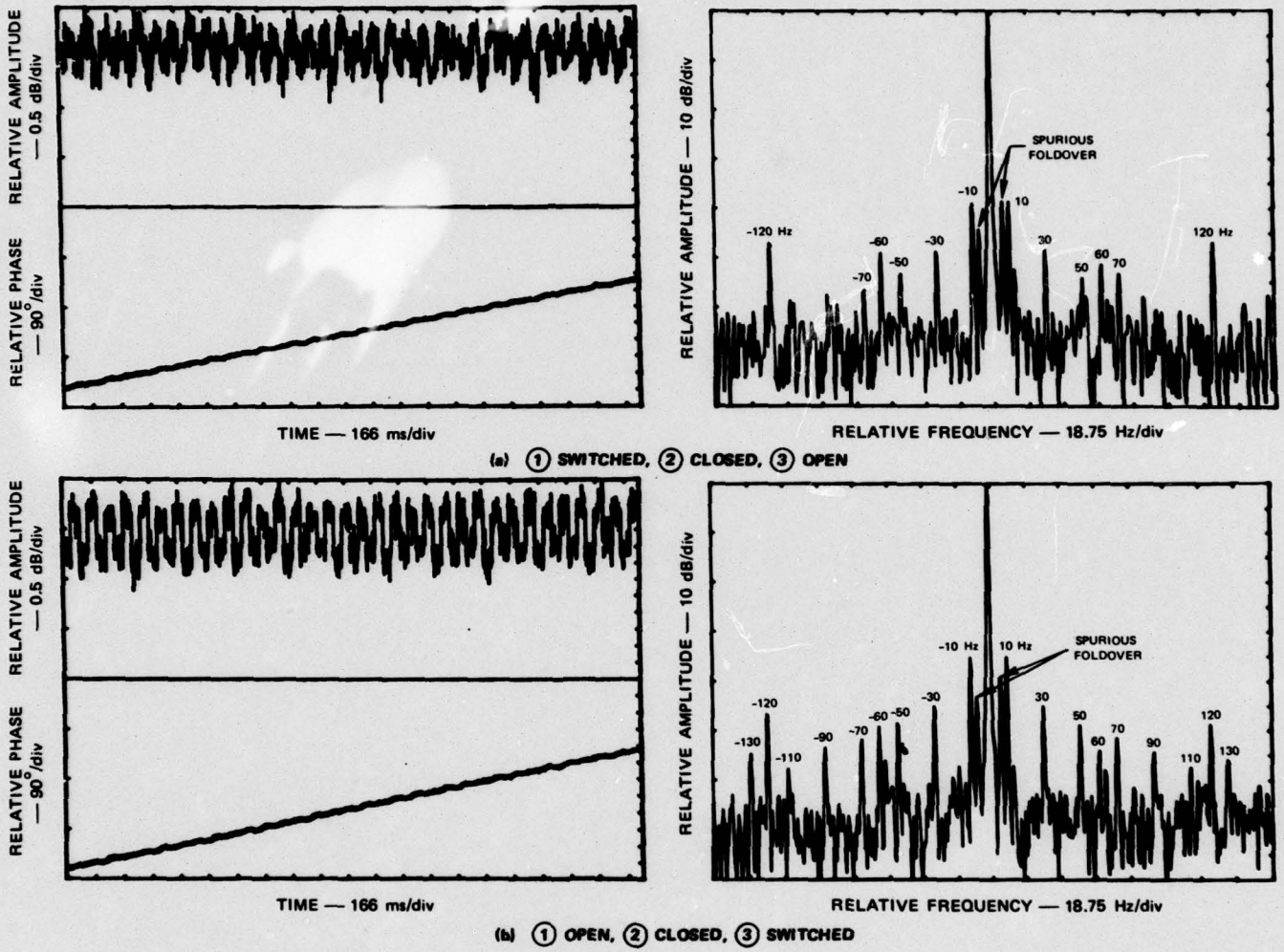


FIGURE 6 MODULATION OBTAINED USING A SINGLE ACTIVE SWITCH

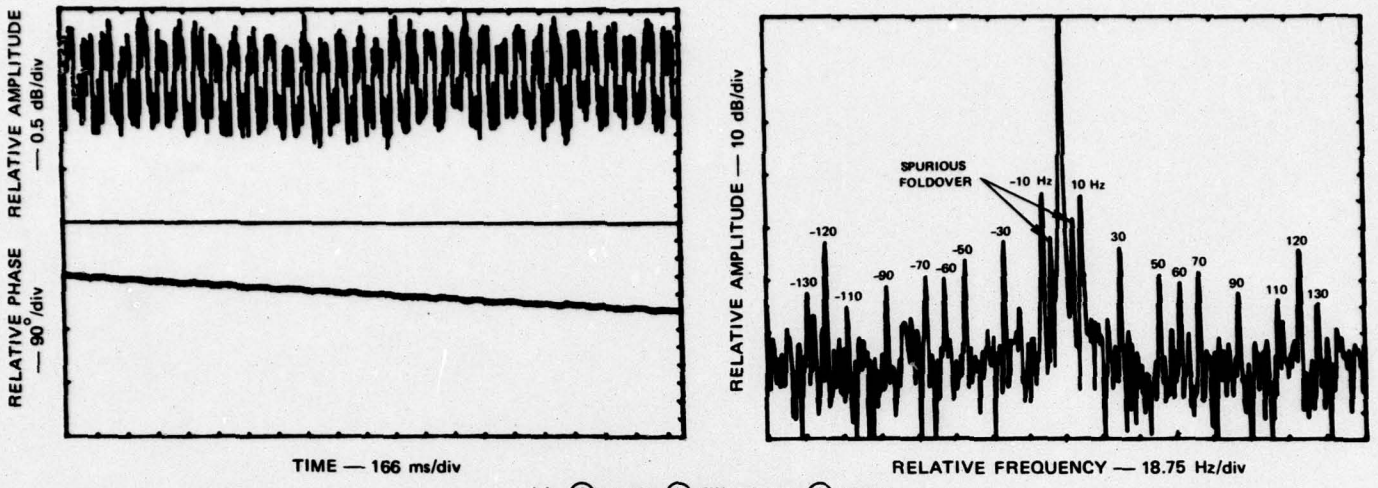


(c) ① OPEN, ② SWITCHED, ③ OPEN

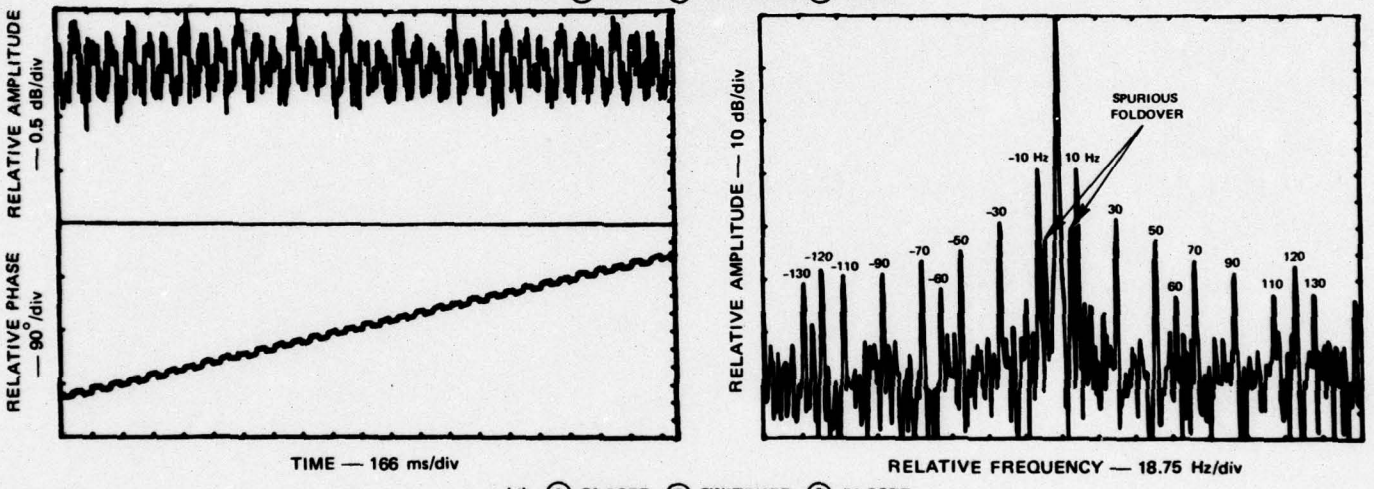


(d) ① CLOSED, ② SWITCHED, ③ CLOSED

SA-4176-11

FIGURE 6 (Concluded)

observed in the spectra. In addition, two types of spurious lines occur in the spectra. One type is the so-called "hum" line that occurs at multiples of the 60-Hz power-line frequency. The other type is a "fold-over" line that results from the gradual roll-off of the band-limiting filter used in recording the data.

Figure 6(a) shows the results obtained when Switch 1 is activated, Switch 2 is closed, and Switch 3 is open (switch numbers are circled in this and succeeding figures). Figure 6(b) shows the case where the roles of Switches 1 and 3 are reversed. Symmetry considerations lead one to expect that these results should be the same. However, we see that the spectral lines are about 4 dB weaker when Switch 1 is activated than when Switch 3 is activated. Inspection of the temporal waveforms shows that the modulation obtained when Switch 1 is activated is indeed less pronounced. We suspect that this result may be caused by differing RF "contact" impedances in the reed switches, but we have not attempted to prove this conjecture.

Figures 6(c) and 6(d) show the effect of switching Switch 2 while maintaining Switches 1 and 3 either open or closed, respectively. In general, we see that Switch 2 produces more spectral energy than does either Switch 1 or 3. Furthermore, Switch 2 produces the most spectral energy when both Switches 1 and 3 are kept closed. From Figure 6(d) we see that this result is due to the increase in phase modulation that accompanies the closing of these switches.

Thus, these experiments demonstrate that the degree of modulation of a scattered signal can depend on contact location, and also on the state of the "resting" contacts.

### 2. Effects of Switching Phase

Assuming that the movements of the contacts on a target are coherently related, it is of interest to consider what effect the relative phases of these movements have on the modulated scattering. For our two-plate scatterer, consider the case where Switches 1 and 3 are switched either in or out of phase. Because of the physical symmetry

in the locations of these switches, we expect that no modulation will be observed when the switching is $180^{o}$ out of phase.

This effect is demonstrated by the results shown in Figure 7. Figure 7(a) shows the case of in-phase switching, and Figure 7(b) shows the case of out-of-phase switching. It is seen that the spectral power is greatly reduced in this latter case.

### 3. Effects of Contact Coherence

So far, we have considered the driving functions for the various switches to be periodic and coherently related. Again, in practice neither of these conditions may be realized.

The experimental results given in Figure 8 illustrate some effects of random switching. In these experiments either one or two random-function generators were used to drive the switches. The outputs of these generators were filtered to limit their signal bandwidths to approximately 20 Hz. Figure 8(a) shows the effect of using only one random source to control both Switches 1 and 3 (with Switch 2 closed). Considerable modulation of the temporal waveform is observed, since both switches are opening and closing at the same times. However, since the switching waveform is a random function of time, the spectral energy is spread out, with, of course, most of the energy being contained within 20 Hz of the carrier frequency. Thus, any information concerning the target that might be contained in such a spectrum is, at best, disguised. On the other hand, it may be possible to gain information about the target more directly from the time-domain waveforms associated with the amplitude and/or phase modulation of the scattered signal. For example, one could measure the amplitudes and positions of the pulses shown in Figure 8(a) and then perform statistical analyses to try to develop relationships among these parameters.

In Figure 8(b) we see the effect of using two independent sources to control Switches 1 and 3. The modulation on the scattered signal is now "more random", since the opening and closing of the two switches no longer necessarily occurs at the same time. Consequently,

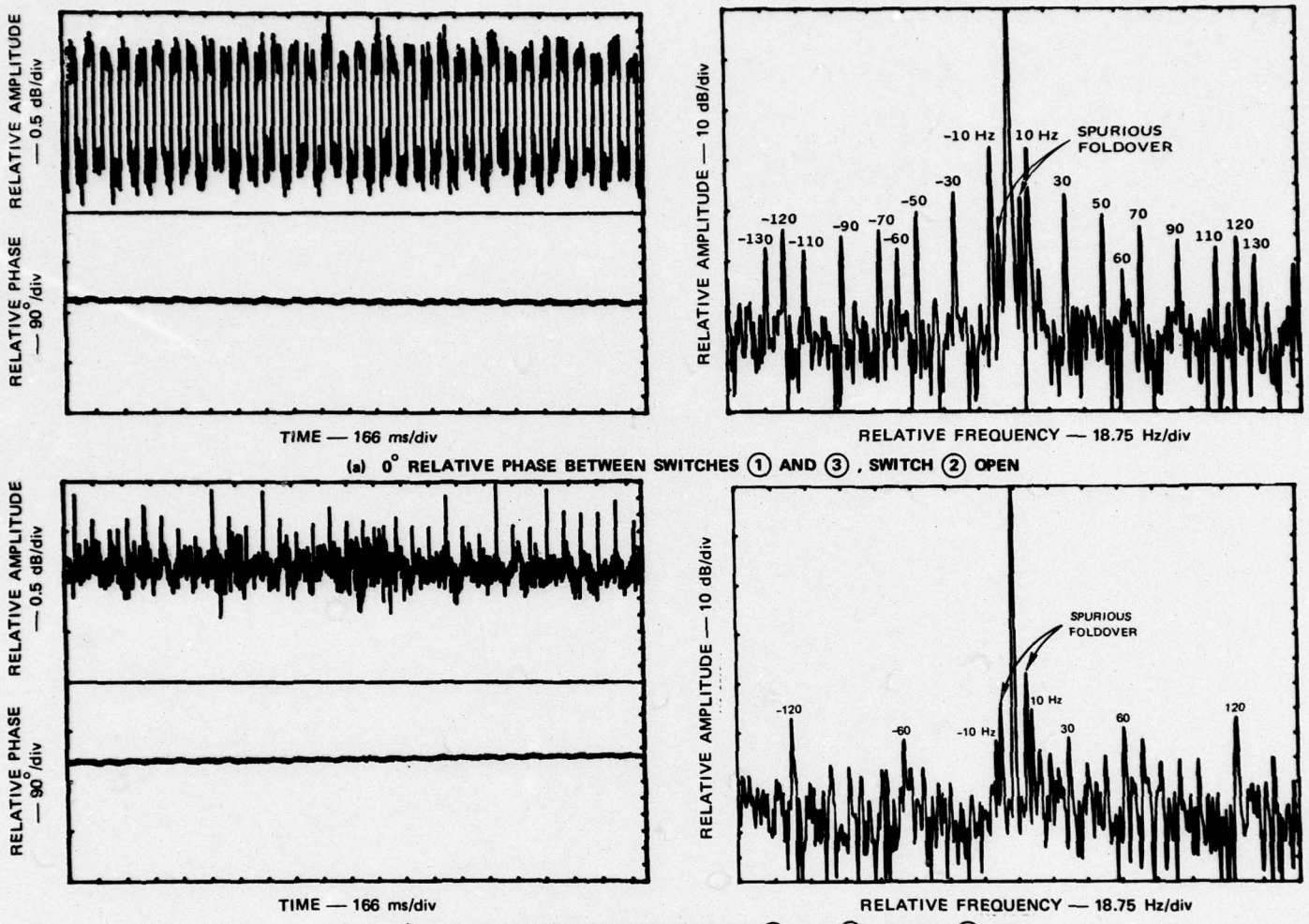


FIGURE 7 MODULATION OBTAINED USING TWO ACTIVE SWITCHES

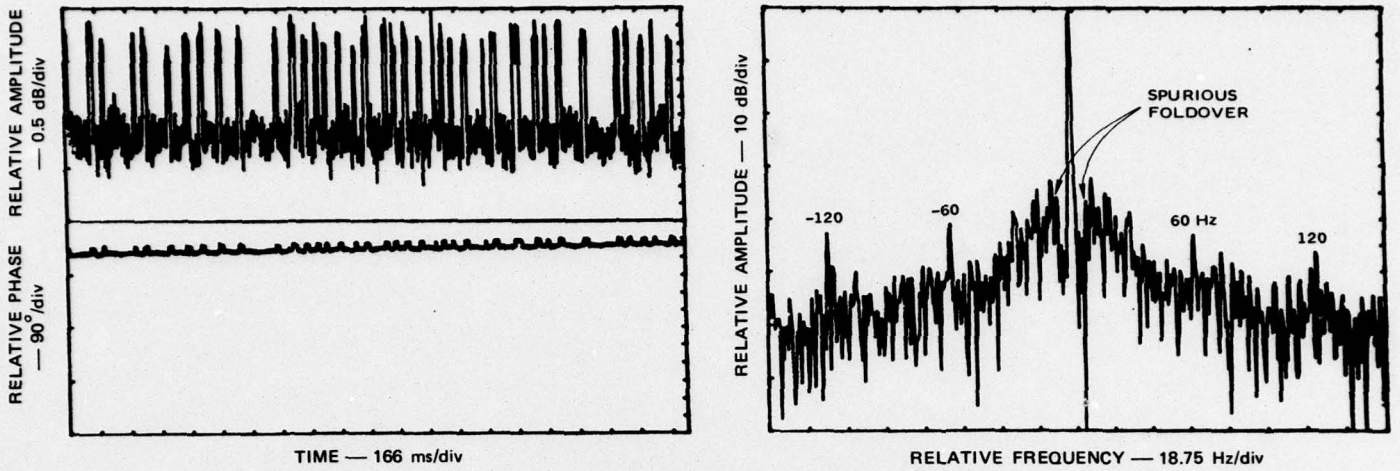


(a) ① AND ③ SWITCHED — SAME SOURCE, ② CLOSED

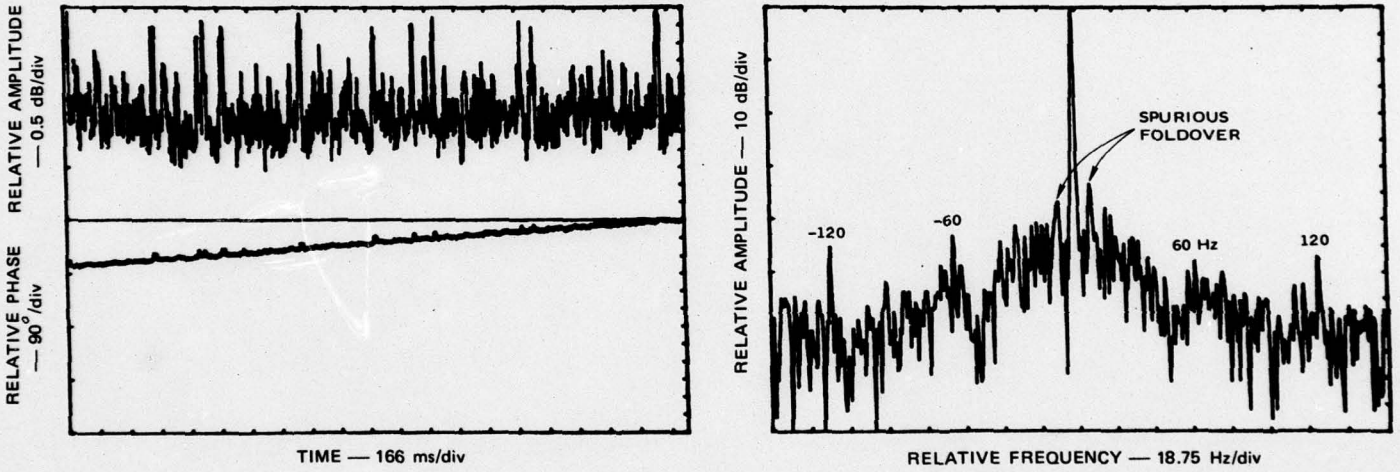


(b) ① AND ③ SWITCHED — SEPARATE SOURCES, ② CLOSED

SA-4176-13

FIGURE 8 MODULATION OBTAINED USING RANDOM SWITCHING

the spectral energy is more spread out in this case, and the derivation of statistically significant parameters from the time-domain data is made more difficult.

## C. Motion of Target Elements

Motion of the individual elements that comprise a target can also modulate the scattered signal. For example, there can be phase modulation due to the Doppler effect caused by the moving elements. However, if the motion is small in terms of a wavelength, this effect is also small. In addition, amplitude modulation can occur because the scattering from a moving element depends on the aspect of the element with respect to the transmitting and receiving directions.

These additional modulations may also be useful for target-identification purposes. However, if all the various possible types of modulation occur together (including intermittent-contact RADAM), the correct interpretation of the result may be difficult to obtain. Thus one would like to be able to separate the various modulations and focus on the one that is most indicative of the target.

In Figure 9 we illustrate the characteristics of two different kinds of modulation that were obtained using the two-plate scatterer shown in Figure 5. In these experiments, Switch 2 was removed and Switches 1 and 3 were connected between the plates by means of flexible beryllium-copper contacts. In the first experiment the two plates were aligned parallel to one another so that good electrical contact was made to the flexible contacts. Then the switches were activated in a square-wave fashion at a rate of about 14 Hz and the modulated backscatter was measured. The results are shown in Figure 9(a). Note that we have improved the bandwidth limiting of the data taken in these experiments so that it is no longer possible to detect spurious foldover lines in the spectra. We see that the rapidity of change inherent in a mechanical metal-to-metal switching process produces spectral sidebands having amplitudes that are consistent with square-wave modulation (of both amplitude and phase).

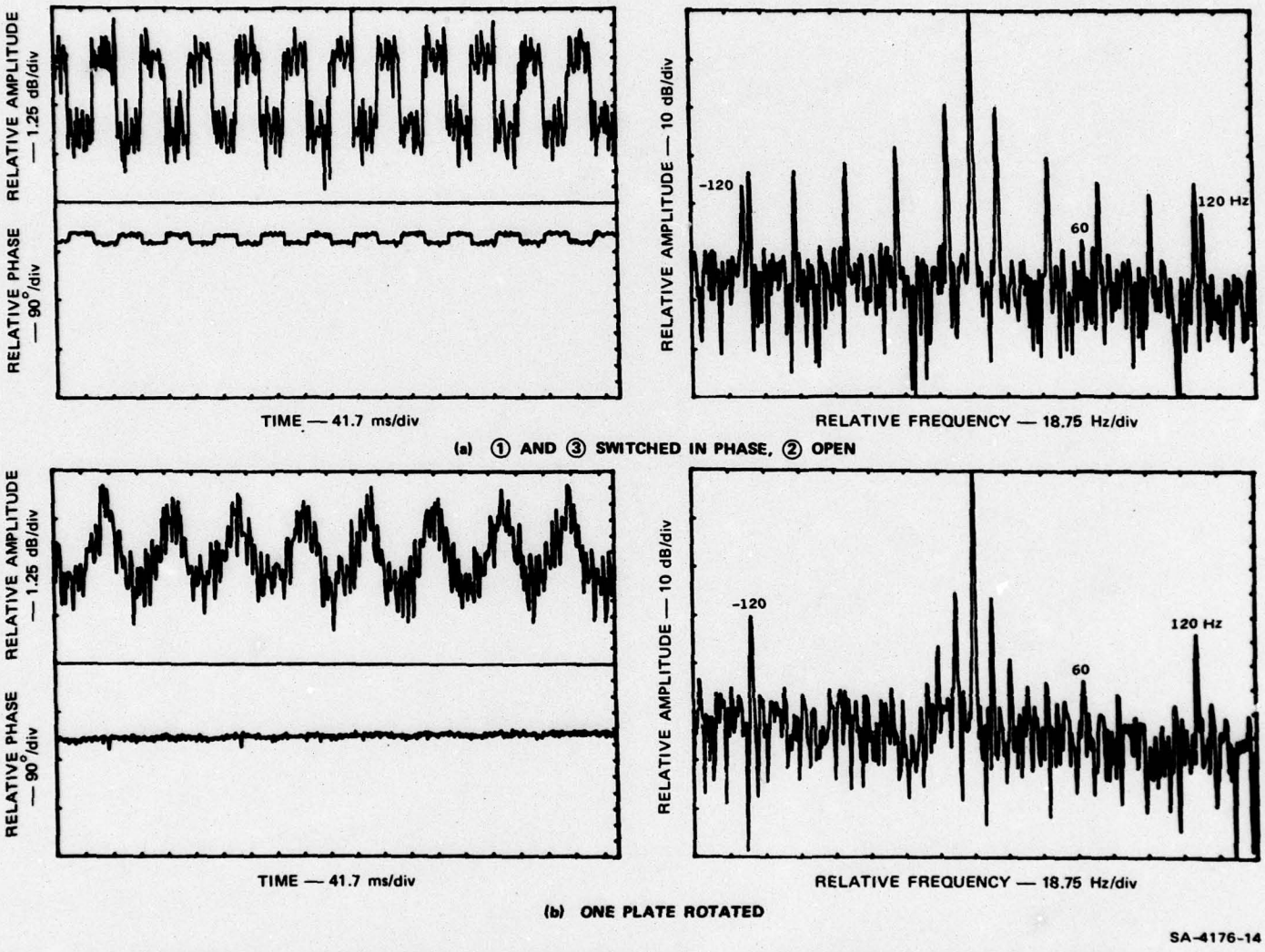


FIGURE 9 COMPARISON OF SWITCHING AND MOTION BETWEEN TARGET ELEMENTS

In the second experiment we opened both of the switches (without removing the target from its support) and rotated one of the plates at five revolutions per second. This produced a periodic amplitude modulation of the scattered signal with a frequency of 10 Hz--these results are shown in Figure 9(b). Because of inertia, movement of a target element having finite mass can never occur as abruptly as a change in metal-to-metal electrical contact, and thus the modulation waveform is more sinusoid-like, rather than square-wave-like. This fact is reflected in the rapid falloff of the corresponding spectral sidebands.

Thus, it should be possible to use the time waveform or its associated spectral characteristics to distinguish between the modulation produced by changing contacts and that produced by motion of a target element. Also, it is possible that one type of target variation will produce more phase modulation than another, as is the case in this example, and this fact could also be used for discrimination.

## D. Effects of Contact Materials

Our conceptual model for intermittent-contact RADAM involves the modification of surface currents on the target by changes in the state of contact between two or more parts of the target. In this model the degree of surface-current modification is dependent on the contact impedance between the touching parts. In real targets one would expect some variation in this contact impedance, depending on the type and condition of the target material(s). Hence we have carried out a series of experiments aimed at assessing the effect of variations in target material.

A photograph of the target used in these experiments is shown in Figure 10. The target is a resonant slot in a metal plate. With this arrangement we can measure the forward scattering through the slot, rather than the backscattering. This scheme provides good isolation between transmitter and receiver when the slot is covered, because they are on opposite sides of a metal plate that is surrounded by a large metal screen and RF absorbing material.

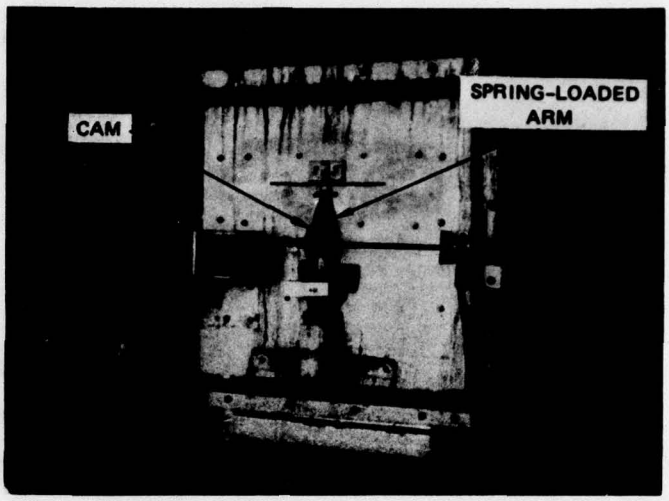


SA-4176-15

FIGURE 10 PHOTOGRAPH OF SLOTTED PLATE WITH MECHANICAL SHORTING ARRANGEMENT

Contact modulation is achieved in this arrangement by periodically short-circuiting the slot at its center. This switching is performed mechanically by using a rotating cam to move a spring-loaded arm up and down with respect to the plate. These mechanical features are visible in Figure 10. The spring-loaded arm is firmly attached to the large metal plate just above the slot, and intermittent contact between the arm and the plate occurs just below the slot. A small, removable contact plate can be attached to the large plate at this point. This arrangement permits contact plates made of different materials to be easily interchanged.

Before carrying out the experiments with different contact materials, we first conducted an experiment to demonstrate that the scattering from a metal target is directly related to the surface currents on the target. Although this relationship is a generally accepted fact, we thought that conducting this experiment would be worthwhile because the use of a modulated target provides a particularly clear demonstration of the relation between surface currents and scattering.

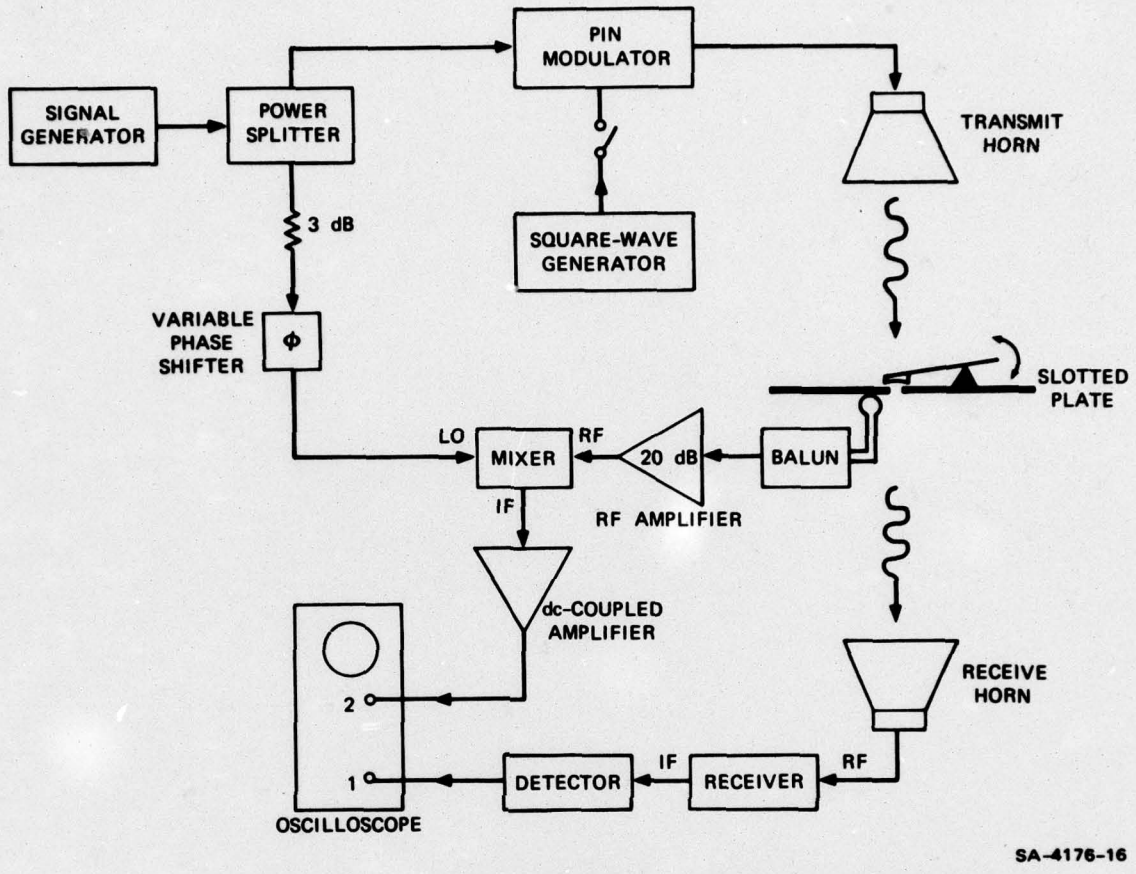


**FIGURE 11 BLOCK DIAGRAM OF EXPERIMENTAL ARRANGEMENT USED FOR COMPARING SCATTERED SIGNAL AND RF SURFACE CURRENT**

A block diagram of the experimental arrangement is shown in Figure 11. Basically, there are two detection systems: One system uses a small shielded loop to sense the surface current on the slotted plate, and the other system uses a conventional receiver to sense the scattered RF signal. The shielded loop was placed on the unencumbered side of the plate (nearest the receiver). The characteristics of the balun were checked carefully to assure that no significant common-mode currents would be picked up by the loop. A photograph of the loop in place near the center of the slot is shown in Figure 12.

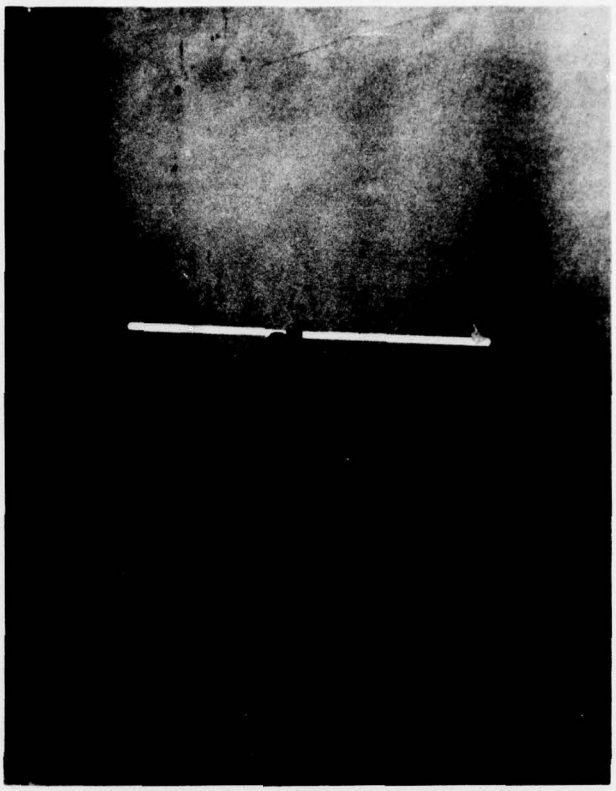

SA-4176-17

FIGURE 12 PHOTOGRAPH OF CURRENT-SENSING LOOP

The experimental procedure was as follows: First, with the contact in the open position, the transmitter was square-wave modulated and the phase shifter adjusted so that the output of the current probe was positive when the transmitter was on. Then the transmitter was operated in a CW mode at 800 MHz and the vibrating contact arm was activated with a repetition rate of 5 Hz. Finally, the outputs of the two sensors were compared on a dual-channel oscilloscope.

Representative experiment results are shown in Figure 13. We see that, as expected, the temporal characteristics of the scattered RF signal and the RF surface currents are identical. Hence, any modification of the surface currents modifies the scattered signal accordingly. The

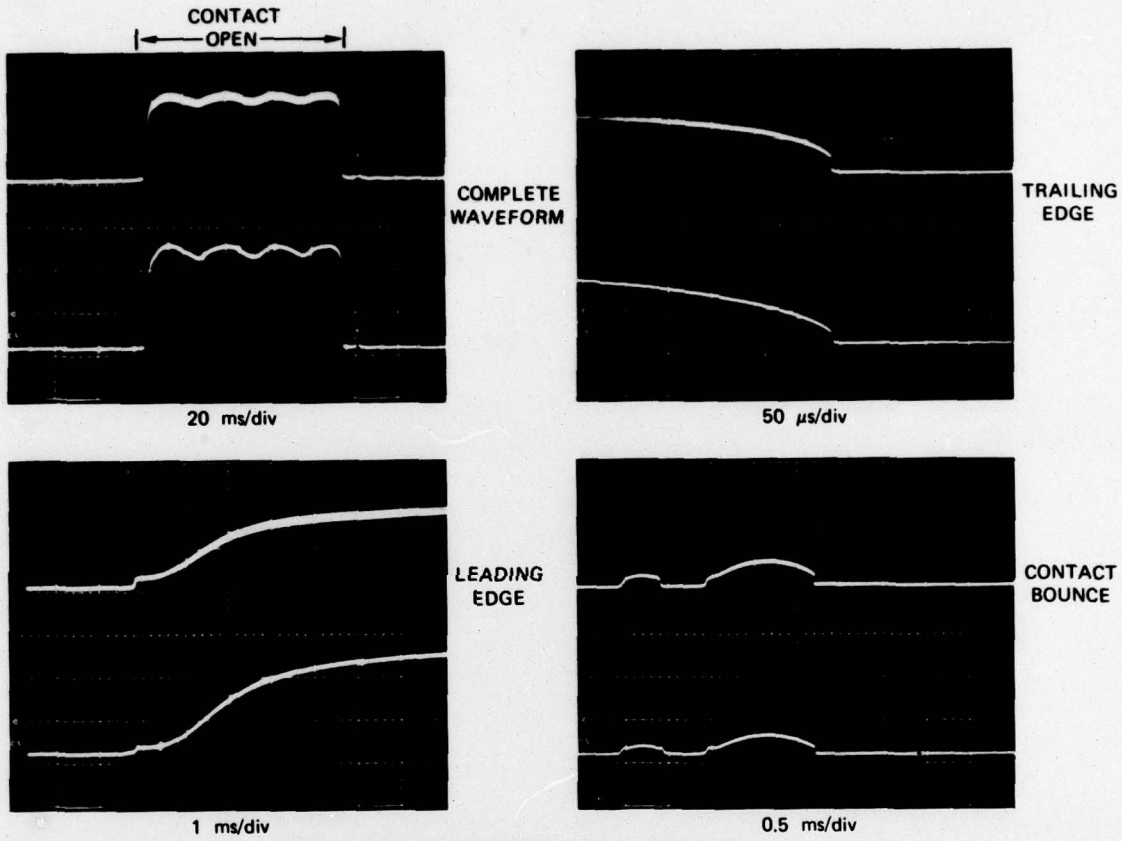


FIGURE 13 COMPARISON OF SCATTERED SIGNAL AND RF CURRENT.

sudden jumps in signal that occur when the contact opens and closes should also be noted. These sharp changes occur because the contact goes from conducting to capacitive and vice versa. It is these sudden changes that provide most of the spectral energy in the intermittent-contact RADAM effect.

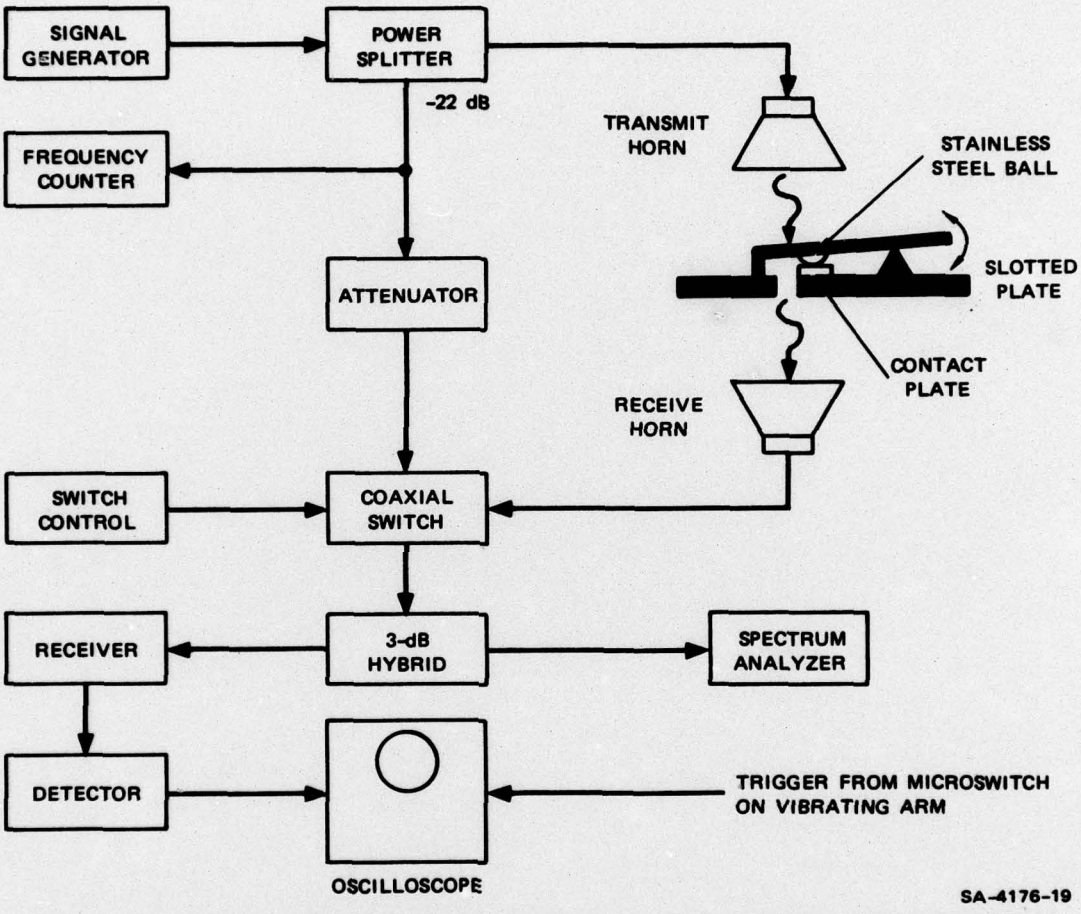


FIGURE 14 BLOCK DIAGRAM OF EXPERIMENTAL ARRANGEMENT FOR COMPARING CONTACT MATERIALS

Now we return to our discussion of the experiments wherein we examined the effect of contact material. The experimental arrangement was modified to that shown in Figure 14. A stainless-steel ball bearing was used for the contact on the vibrating arm in order to minimize variations

in contact area caused by flexing of the arm or variations in the thickness of the contact plates. The ball was connected through the arm to the opposite side of the slot by means of a low-inductance conductor. The frequency and available output power of the signal generator were kept constant throughout the series of experiments at 750 MHz and +2.5 dBm, respectively. With this level of incident power, the power received through the open slot was -52 dBm. The frequency of vibration of the contact was 2.5 Hz, and the thickness of all the contact plates was about 0.030 inch.

A number of contact materials were tested; a list of these materials is given in Table 1. Also shown in this table is the corresponding change in forward-scattered power that occurs when the contact goes from the open to the closed state. We can immediately conclude from these results that the modulation caused by a vibrating contact is about the same for all metals if their surfaces are good conductors. We also see from the data that nonconducting paint or a heavy oxide such as rust causes a significant reduction in the modulation.

Table 1

MATERIALS TESTED AND CORRESPONDING CHANGES IN FORWARD-SCATTERED POWER

| Material | Change in Received Signal Level From Open to Closed States (dB) |
|---|---|
| Copper | -15.5 |
| Aluminum | -15.9 |
| Brass | -15.3 |
| Cold-rolled steel | -15.6 |
| Stainless steel | -16.0 |
| Galvanized steel | -15.2 |
| Slightly rusted cold-rolled steel | -15.1 |
| Very rusted cold-rolled steel | - 6.8 |
| Cold-rolled steel with acrylic paint | - 5.4 |
| Copper with silicon grease | -14.2 |
| Plastic (NEMA grade G-10) $\varepsilon_r = 4.9$ | - 1.4 |

It is also informative to examine the behavior of the contact modulation in the time domain. Figure 15 shows two examples for good conductors--namely, copper and aluminum. The waveforms are essentially the same--the slight difference in the duration of the closed state is due to a slight difference in the thicknesses of the contact plates.

Next, in Figure 16, we compare the effects of various surface conditions for a cold-rolled-steel contact plate. As mentioned previously, we see that rust and paint reduce the change in scattering caused by closing the contact. In addition, we see that a rusted contact behaves somewhat erratically. A similar erratic behavior can occur even when the surface oxide is thin, as in aluminum, if the contact pressure is light. This effect is illustrated in Figure 17.

As a matter of interest, we also took electron micrographs of the contact areas for some of the different contact materials. The relevant photographs for copper, aluminum, and rusted cold-rolled steel are shown in Figure 18. We can see that the aluminum oxide has been broken through by the contact, but that the iron oxide is obviously too thick for this to happen.

Thus, we see that the nature of the contact materials can influence the intermittent-contact RADAM effect through two major parameters: (1) the amount of amplitude and phase change between open and closed states, and (2) the time scale of the change. The observed differences between materials can be related to whether a low-resistance contact is formed, or to whether an oxide or other intervening material prevents the formation of such a contact.

## E. VHF Scattering from a D8 Tractor

Up to this point in our studies we had been dealing entirely with simple targets in a controlled laboratory environment. We therefore became interested in performing some qualitative scattering measurements on a moving target having intermittent contacts so that we could get some idea of what modulation characteristics we might expect for a "real" target.

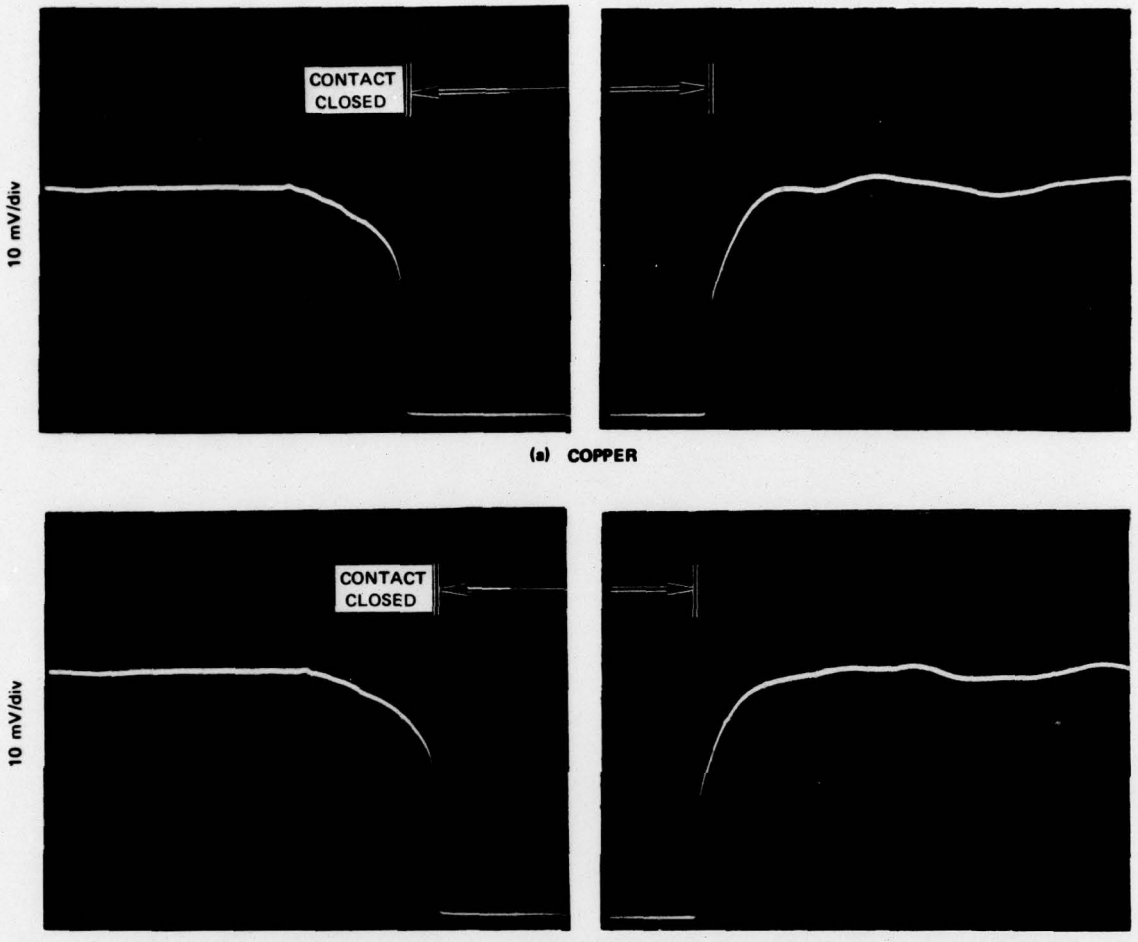


FIGURE 15 DETECTED FORWARD SCATTERING AS A FUNCTION OF TIME FOR LOW-RESISTANCE CONTACTS

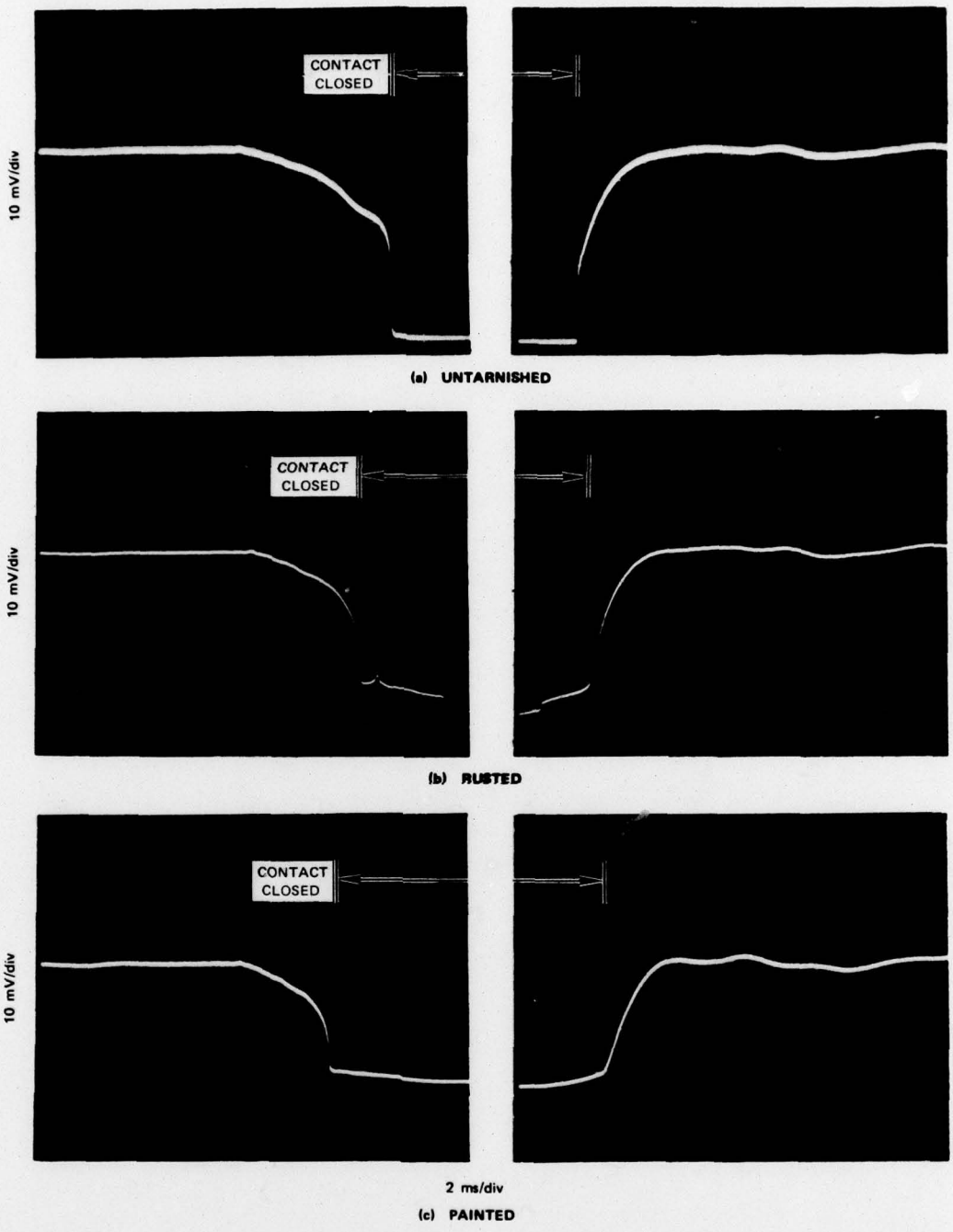


FIGURE 16 DETECTED FORWARD SCATTERING AS A FUNCTION OF TIME FOR A COLD-ROLLED-STEEL CONTACT PLATE

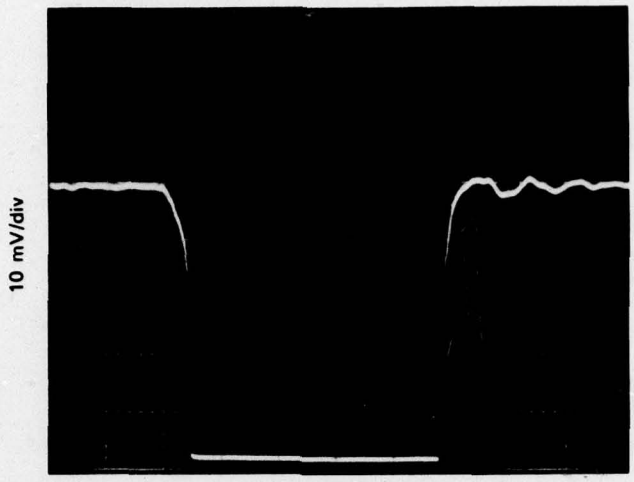


(a) HEAVY PRESSURE


(b) LIGHT PRESSURE

SA-4176-22

FIGURE 17 DETECTED FORWARD SCATTERING AS A FUNCTION OF TIME FOR AN ALUMINUM CONTACT PLATE

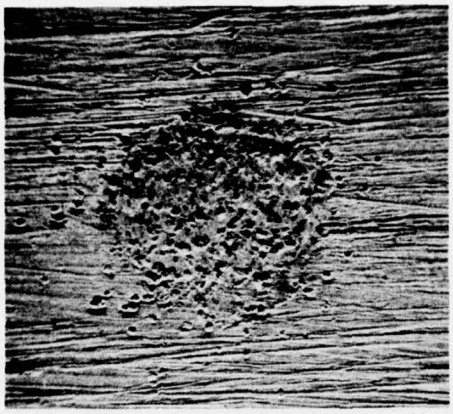

(a) COPPER

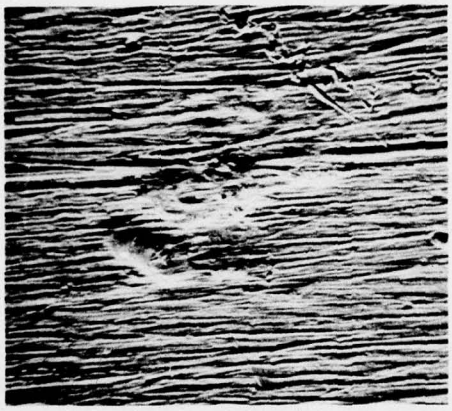

(b) ALUMINUM

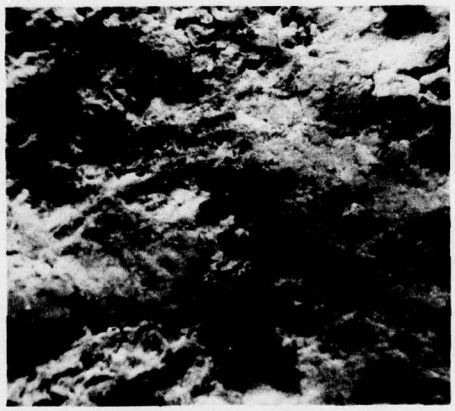

(c) RUSTED COLD-ROLLED STEEL

SA-4176-23

FIGURE 18 ELECTRON MICROGRAPHS OF CONTACT AREAS (200X)

For these experiments we selected a D8 Caterpillar tractor, which is a large earth-moving tractor having many vibrating and moving parts. We set up a CW bistatic radar near a large field and ran the tractor over a course that was within the coverage area of the radar. We chose an operating frequency of 50 MHz so that the dimensions of the tractor would be on the order of one-half wavelength. The transmitting and receiving polarizations were aligned vertically with respect to the earth. The data were recorded on analog tape using 6 kHz of bandwidth.

Some illustrative results obtained by digitizing the data and performing complex demodulation and spectral analysis are shown in Figure 19. For reference, Figure 19(a) shows the amplitude and phase of the scattered signal, and its spectrum, as functions of time for the case where the tractor is stationary, but with its motor running. The spectrum is shown as a function of time since the scattered signal will change as the target moves, as will the modulation carried by the signal. The frequency resolution in this spectral display is about 5 Hz.

Some data obtained with the tractor moving cross-range at about 10 mph is shown in Figure 19(b). We see that the tractor motion produces a weak amplitude modulation having a frequency of about 19 Hz. This modulation appears to be sinusoid-like, thus indicating that the source of the modulation is a moving target element rather than an intermittent contact. The most likely candidate for this element is a tread, or group of treads, on the vehicle track. In addition, there is a noticeable increase in the impulsive noise on the scattered signal when the vehicle is moving. It likely that the source of this noise is the multitude of intermittent contacts that exist on this type of vehicle.

The spectra in Figure 19(b) show some spreading due to the motion-induced modulation. However, with the degree of frequency resolution inherent in this display, it is difficult to determine whether any corresponding spectral lines exist for any significant period of time. A better display for this purpose would be a frequency-versus-time plot where the spectral amplitude is displayed as a gray scale.

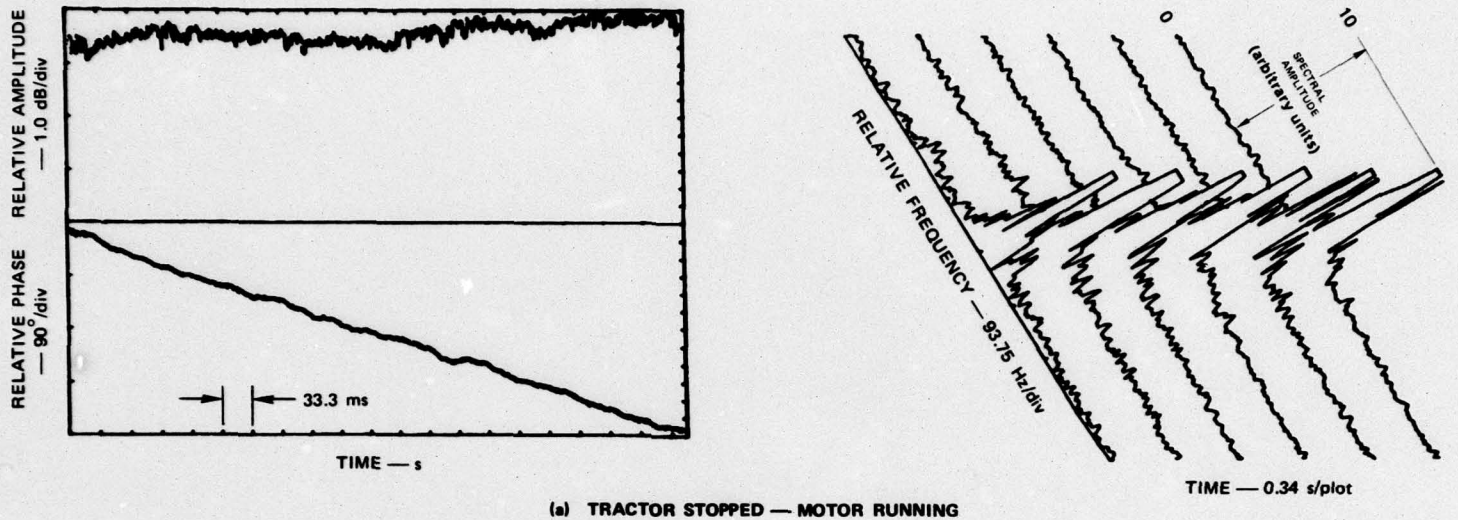


(a) TRACTOR STOPPED — MOTOR RUNNING

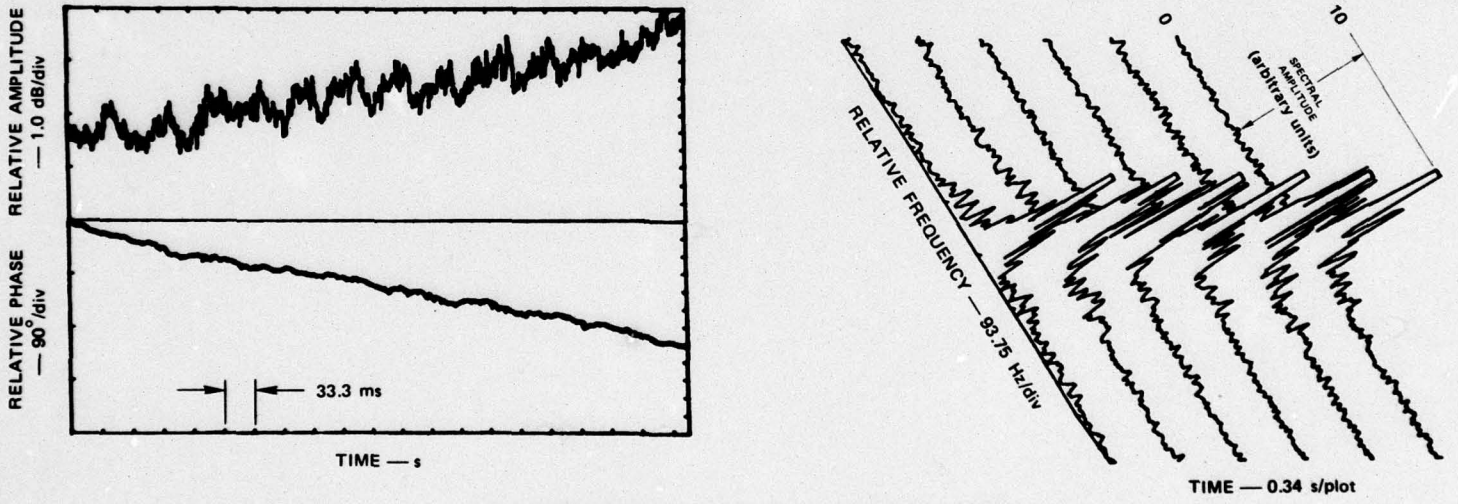


(b) TRACTOR MOVING AT 10 MPH — BROADSIDE ASPECT

SA-4176-24

FIGURE 19 TEMPORAL AND SPECTRAL DATA FOR VHF SCATTERING FROM A D8 TRACTOR

These results give a good indication of the difficulties that one will face in attempting to detect and interpret the intermittent-contact modulation on the scattering from a complex target. However, it appears that the knowledge we have gained from our laboratory studies will be a definite aid to such an endeavor.

# III CONCLUSIONS

Our work during the first year of this contract succeeded in establishing a basic approach for modeling the intermittent-contact RADAM effect--namely, we have shown that the effect is due to variations in surface currents caused by contact motion, and thus can be described using a loaded-scatterer model. During this second year of work we have studied various facets of the effect in an effort to improve our understanding of the factors that affect the observed backscatter signature obtained from a target having intermittent contacts. The major conclusions derived from this recent work are:

- The RF frequency dependence of the scattered spectral energy produced by intermittent contacts is determined by (1) the ratio of the target dimensions to the electromagnetic wavelength, and (2) the frequency dependence of the impedances associated with the contacts on the target.
- The observed modulation on the backscattered signal depends on the locations of the contacts within the target and also on their phasing.
- If the forces that produce contact motion are seemingly random functions of time so that spectral analysis is not particularly useful, it may still be possible to gain information about the target by performing various statistical analyses on the time-domain waveforms. Success with this approach in the case of multiple contacts will depend in part on whether the motion of the contacts is coherent--i.e., on whether the contacts act in concert or not.
- Modulation produced by the motion of target elements can be identified by its sinusoid-like nature; modulation produced by intermittent contacts is more like a square wave. It may be possible to separate these two types of modulation by using differences in their spectra or in their phase signatures.
- The nature of the materials that form the contacts in the target can influence the intermittent-contact RADAM effect through two major parameters: (1) the amount of amplitude and phase change between open and closed states, and (2) the time scale of the change. The observed differences between materials can be related to whether a low-resistance contact is formed, or to whether an oxide or other intervening material is present instead.

## REFERENCES


1. R. F. Harrington, "Theory of Loaded Scatterers," Proc. IEE (London), Vol. 111, pp. 617-623 (April 1964).

2. Y. Hu, "Back-scattering Cross Section of a Center-Loaded Cylindrical Antenna," IRE Trans. on Antennas and Prop., Vol. AP-6, pp. 140-148 (January 1958).